

Spin-orbit coupling mediated tunable electron heat capacity of quantum wells

Parijat Sengupta¹ and Enrico Bellotti¹

*Dept. of Electrical Engineering and Material Science Division
Boston University, Boston, MA 02215.*

The heat capacity of conduction electrons obtained from the Sommerfeld expansion is shown to be tunable via the Rashba and Dresselhaus spin-orbit coupling parameters. Using an AlInSb/InSb/AlInSb as a representative heterostructure with alterable well and asymmetric barrier regions, the heat capacity is found to be higher for the spin-down electrons and suffers a reduction for wider wells. A further lowering is obtained through the application of an uniaxial strain. Finally, we suggest a method to determine the spin lifetimes for spins relaxing via the D'yakonov-Perel' mechanism from experimental estimates of thermodynamic potentials such as the Helmholtz free energy and the heat capacity.

The electronic contribution to the specific heat is usually masked by the phonon component or the lattice specific heat and becomes the dominant term only in the low-temperature regime. The specific heat measured much below the Debye and Fermi temperatures follows a relationship of the form $\gamma T + \beta T^3$, the T^3 contribution arising from lattice vibrations while the electrons contribute linearly in T .¹ The electronic contribution is further reduced as few electron states are available in the thermal interval of the order $k_B T$ around the Fermi energy. However, at sufficiently low temperatures, the measurement of the electronic specific heat unveils details about elementary excitations including features of the density of states close to the Fermi level, furnishing quantitative insight to several key microscopic processes. The many-body interactions in a strongly correlated Fermi liquid, for instance, is characterized by the deviation of Wilson's ratio (the ratio of the magnetic susceptibility to specific heat divided by temperature) from unity for weakly correlated electrons.² From a broader perspective, the laws of thermodynamics and statistical mechanics have been applied to explain the behaviour of a diverse body of phenomena such as Luttinger liquids, superfluidity, and superconductivity. Experimental groups routinely record data on the specific heat of superconductors to probe the superconducting energy gap, the order parameter symmetry, and the quasi-particle density of states.³

In this letter, in contrast to experimental measurements, we perform a theoretical determination of the electron heat capacity at constant volume, C_v , of conduction electrons confined in the well region of zinc blende heterostructures grown along [001]-axis and show their tunability under extrinsic spin-orbit interactions. The tunability and optimization of heat capacity is fundamental to the design and the dynamic response of sensor materials, for e.g., thermal CMOS microtransducers, thermocouple thermometers, and low temperature sensors for ultra-scaled integrated circuits. We show that the heat capacity is affected by the heterostructure setup whereby a wider well region reduces the C_v with the possibility of additional tuning through uniaxial strain which further lowers it. As an adjunct, we suggest a possible experimental method that facilitates the retrieval of spin lifetimes from experimentally recorded electron heat capacity and allied thermodynamic potentials.

For low temperatures that comply with the criterion, $k_B T \ll T_F$, where $k_B = 8.617 \times 10^{-5} \text{ eV K}^{-1}$ is the Boltzmann constant and T_F represents the Fermi temperature, the C_v can be reasonably approximated using the Sommerfeld expansion.¹ We begin by examining this quantity for conduction state electrons described by a parabolic dispersion and spin-split by the Rashba and Dresselhaus spin-orbit interaction (SOI).⁴ The Rashba SOI manifested as splitting of energy bands typically originates in non-centrosymmetric crystals or structures with miscut surfaces, collectively referred to as structural inversion asymmetry (SIA). It is a remarkably adjustable phenomenon vital to the control and production of spin-polarized currents in spin-based devices. The Dresselhaus splitting on the other hand is intrinsic to the crystal and is generally an invariant parameter typically much smaller than Rashba SOI. Since these SOI mechanisms reorganize the electron energies, a concomitant effect on the C_v must exist. To see this, observe that a direct application of the Sommerfeld expansion leads to an SOI-governed density-of-states (DOS) dependent expression for the internal energy density (U) from which we extract the heat capacity using $C_v = \partial U / \partial T$. It follows that the C_v is spin-dependent. Note that heat capacity always refers to a per unit area quantity.

We begin with an ensemble of conduction electrons in ZB quantum wells that are modeled assuming a parabolic dispersion with spin-orbit interaction terms. For ZB, the Hamiltonian has the form:

$$H_{zb} = \frac{p^2}{2m^*} + \lambda_R (\sigma_x k_y - \sigma_y k_x) + \lambda_D \langle k_z^2 \rangle > (\sigma_x k_x - \sigma_y k_y), \quad (1)$$

where $\lambda_R > 0$ and $\lambda_D > 0$ are the Rashba and Dresselhaus coupling parameters, respectively and the condition $\lambda_R \neq \lambda_D$ holds for all cases. The cubic dependencies of the form $k_x k_y^2 \sigma_x - k_y k_x^2 \sigma_y$ in the Dresselhaus Hamiltonian have been ignored while the k_z and k_z^2 terms have been replaced by their quantized values 0 and $(\pi/L)^2$. The width of the quantum well is L in appropriate unit. The dispersion relationship for the chiral bands of ZB conduction electrons using Eq. 1 is $\hbar^2 k^2 / 2m \pm \beta k$. The coefficient β takes the form $\beta = \sqrt{(\lambda_R^2 + \lambda_D^2 + 2\lambda_R \lambda_D \sin 2\theta)}$ and $\theta = \tan^{-1} k_y / k_x$. Note that the effective mass in the above expressions is m^* which we obtain for sev-

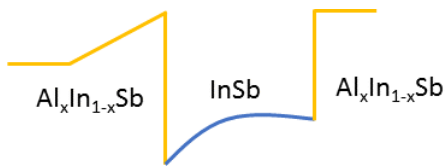


FIG. 1. Schematic of the asymmetric InSb quantum well surrounded by $\text{Al}_x\text{In}_{1-x}\text{Sb}$ barriers of variable width and alloy composition. The dissimilar barriers flanking the quantum well induces a stronger SIA and enhanced Rashba splitting.

eral cases discussed later from relevant k.p Hamiltonians. For brevity, we will represent the eigen energies as $\varepsilon(k) = \alpha k^2 \pm \beta k$ where $\alpha = \hbar^2/2m$. The eigen energies are chosen such that $\varepsilon > 0$. For numerical calculations, our representative ZB quantum wells are InSb quantum wells (see Fig. 1) surrounded by asymmetric $\text{Al}_x\text{In}_{1-x}\text{Sb}$ barriers. The reason to select InSb as the well material lies in its narrow band gap, small effective mass, large g -factor, and a significantly large spin-orbit coupling (SOC).

To probe the tunability of the electron heat capacity, we first note that electron energy, U , following the Sommerfeld expansion around the Fermi level ($E = \mu$) is

$$U(T) = \int_{-\infty}^{\mu} ED(E) dE + \eta \frac{\partial}{\partial E} (ED(E)), \quad (2)$$

where $\eta = (\pi k_B T)^2/6$. The DOS, $D(E)$, is considered invariant to ambient conditions if temperature-induced variations to the band structure which are usually insignificant are ignored. Notice that the Sommerfeld relation (Eq. 2) is not exact and we have chosen to ignore higher order temperature contributions. From Eq. 2, the electronic contribution to the specific heat is $C_v = \frac{\partial U}{\partial T} = \frac{\pi^2}{3} k_B^2 T D(E)$. The DOS in Eq. 2 can be calculated employing the standard result $D(E) = \frac{1}{4\pi^2} \int d^2k \delta(E - \varepsilon(k))$. Evaluating the integral gives $D(E) = \frac{1}{4\pi^2} \int_0^{2\pi} d\theta \frac{k_i}{|-2\alpha k_i \mp \beta|}$, where k_i is a root of the equation $g(k) = E - \alpha k^2 \mp \beta k$. The upper (lower) sign is for the spin-up (down) branch. Here, two notable outcomes must be brought to attention: 1) The spin-down (-) branch has a larger DOS and therefore a higher population of electrons than the spin-up (+) branch. 2) The Fermi energy depends on the strength of the Rashba and Dresselhaus coupling parameters; doping apart, the spin-parameters can be used to reset the Fermi energy. As an illustration, through a numerical integration the DOS (and the connected dispersion) for the two spin split energy bands for an InSb quantum well of width $L = 10.0 \text{ nm}$ is plotted in Fig. 2. To clearly show the spin splitting, the Rashba parameter was artificially set to 0.4 eV \AA and the Dresselhaus parameter was chosen to be $(\pi/L)^2 \times 0.48 \text{ eV \AA}^3$. Notice how with increasing energy, the DOS asymptotically approaches a constant value, which is the observed behaviour for a

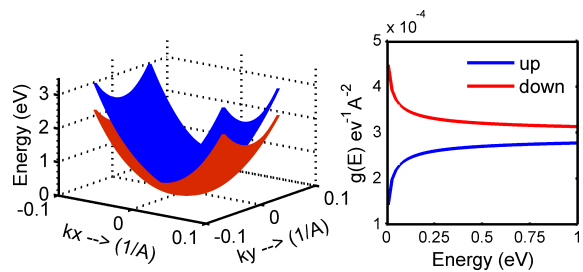


FIG. 2. The eigen energies using Eq. 1 is shown as a surface plot (left panel) along with the corresponding DOS for the two spin-split states. Note that at large values of energy when the αk^2 term in the Hamiltonian is dominant, the DOS assumes a constant number in accord with the result for a 2D system. In calculating the eigen energies and DOS, effective mass was assumed to be $0.014m_0$, where m_0 is the free electron mass.

two-dimensional system. For quantitative expressions to supplement this discussion, see the section on Fermi energy, Ref. 5.

The heat capacity C_v , using the Sommerfeld expansion, is therefore

$$C_v = \frac{k_B^2 T}{12} \int_0^{2\pi} d\theta \frac{k_i}{|-2\alpha k_i \mp \beta|}. \quad (3)$$

The upper (lower) sign gives the heat capacity for the ensemble of spin-up (down) electrons. The tunability of the heat capacity arises from the variable Rashba coupling coefficient and the conduction electron effective mass which enters the DOS expression. In particular, the strength of the Rashba coupling coefficient is $\lambda = \lambda_0 \langle E(z) \rangle$, where $\langle E(z) \rangle$ serves as the average electric field. The material-dependent λ_0 is given as⁶

$$\lambda_0 = \frac{\hbar^2}{2m^*} \frac{\Delta}{E_g} \frac{2E_g + \Delta}{(E_g + \Delta)(3E_g + 2\Delta)}. \quad (4)$$

In Eq. 4, the band gap at Γ is E_g , the spin-orbit splitting is Δ and m^* is the effective mass at points in momentum space close to Γ . The band gap and effective mass are obtained by diagonalization of Kane's eight-band Hamiltonian adapted for heterostructures.⁷ The $k.p$ parameters in Ref. 8 have been used. The effective mass and the band gap evidently change with confinement and external perturbations, such as mechanical strain, which in turn regulates the α_0 parameter. Further, notice that the Rashba coupling parameter is directly linked to the intrinsic spin-orbit coupling and is enhanced by a reduction in the effective band gap, E_g . A pronounced SOC, for instance, in the layered polar semiconductor BiTe ^{9,10} or a strong local electric field, such as the one discovered in the cubic perovskite strontium titanate (SrTiO_3) give rise to large energy splittings of the order 100.0 meV .¹¹ It is useful to bear in mind that while a finite Rashba SOC is usually found in asymmetric crystals, a localized asymmetry arising from strain or a strongly confined impurity can also induce a discernible Rashba splitting as reported for the centrosymmetric layered material 2H-WSe_2 .¹² Lastly, notice that the electric field acting via

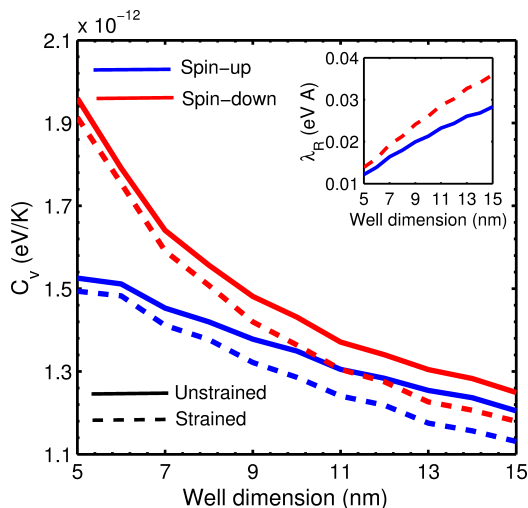


FIG. 3. The calculated heat capacity of conduction electrons for varying InSb well dimensions flanked by AlInSb alloy (see Fig. 1). The Fermi energy was set to $\epsilon_f = 4.0 meV$ and temperature is $T = 5 K$. Note that the Fermi temperature $T_f (\epsilon_f/k_B) = 46 K \gg T$ which renders the Sommerfeld expansion valid. The inset shows the Rashba parameter calculated using Eq. 4.

the gate adjusts the strength of the Rashba coefficient; for numerical calculations the electric field has been set to $10^6 V/m$, a value achieved either through an external bias or doping.

An adjustable asymmetry therefore can alter the RSOC which in turn (this follows directly by an examination of Eqs. 3, 4) manifests in a variable heat capacity. In our simulations, the asymmetry inducements are supplied through strain, dimensional confinement, and an irregular heterostructure configuration (see Fig. 1). The asymmetry through the heterostructure is introduced by employing variable widths and alloy composition (x) for the left and right barrier ($Al_xIn_{1-x}Sb$) while a uniaxial strain further accentuates the underlying crystal order. The effective band gap in Eq. 4 is primarily modulated through multiple dimensional confinement widths. For purpose of calculation, the mole fraction for left- and right-barriers have been set to 0.25 and 0.45, respectively while the well widths are also dissimilar to magnify the local asymmetry. A stress of 1.5 GPA acts along the [001]-axis. For detailed band structure calculations, see Ref. 5 and Ref. 13. With this in mind, let's now examine Fig. 3 which plots the electron heat capacity for heterostructures with well (InSb) regions of varying confinement. The alloyed barrier on the left (right) of the well is 5.0 (7.0) nm and the molar composition (x) was set to 0.25 (0.55).

Firstly, we notice that the Rashba parameter, λ_R , is sensitive (see inset, Fig. 3) to dimensional confinement and strain; an increase in the well dimension and uniaxial strain enhances it. To explain this increase, recall that strain builds up asymmetry within the heterostructure augmenting λ_R , while a wider well region has smaller

band gap entailing a stronger SOI. A stronger SOI is a cause for enlarged Rashba splitting.¹⁴ The boost to the Rashba splitting induced through strain and confinement, however, manifests as a change to the DOS; the DOS for the spin-up states show a decrease while their spin-down counterparts have a reverse behaviour (see Eq. 3 and a short discussion therein, Ref. 5). A straightforward manifestation of this is the ascendancy of the heat capacity for the spin-down electrons over the oppositely spin-polarized set, since the former has a higher DOS, an entity that directly links to heat capacity through Eq. 3. We also observe that the well dimension impacts the C_v which is borne out by the fact that the effective mass of conduction electrons and consequently the DOS is adjusted; a wider well has lower effective mass yielding a lower DOS and therefore a lower heat capacity. It is thus evident that a tuning of the heat capacity to a desired level can be achieved through an application of strain or a choice of heterostructure dimensions; both of which modify the DOS through changed effective mass and the Rashba parameter. A more dynamic method, however, is to alter the Rashba coupling strength ($\lambda_R = \lambda_0 E$) through an external gate bias.

The tunability of the electron heat capacity under spin-orbit interaction has been the main focus of this letter; however, we can also turn the argument and instead ask if it is feasible to retrieve any observable from a direct measurement of the heat capacity. This part is motivated by recent measurements¹⁵ of an exceptionally high heat capacity, reflected in a large effective mass, in compounds collectively called heavy fermion systems. In line with such measurements, we suggest that a similar observable, the spin lifetime, can be determined from experimentally available heat capacity data. For a spin-ensemble relaxing via the D'yakanov-Perel' (DPM) mechanism, the average spin equation is¹⁶

$$\langle \dot{S}_i \rangle = -\tau_p \left[\langle \Omega^2 \rangle \langle S_i \rangle - \sum_j \langle \Omega_i \Omega_j \rangle \langle S_j \rangle \right]. \quad (5)$$

In Eq. 5, the spin precession frequency is $\Omega(k)$ and the momentum relaxation time τ_p is independent of energy. In general, spins relax via DPM in the diffusive limit when the momentum relaxation time is considerably lesser than for a complete spin rotation on the Bloch sphere. For a two-dimensional spin ensemble that precesses under the combined spin-orbit magnetic field of Rashba and Dresselhaus interaction, the $\Omega(k)$ dependence in each case is $\Omega_R(k) = \lambda_R(k_y, -k_x)$ and $\Omega_D(k) = \lambda_D(k_x, -k_y)$, respectively. The spin dephasing tensor by substituting the spin precession components in Eq. 5 for an asymmetric quantum well grown along (001)-axis is¹⁷

$$\frac{1}{\tau_z} = \frac{\tau_p k^2}{\hbar^2} (\lambda_R^2 + \lambda_D^2); \quad \frac{1}{\tau_{\pm}} = \frac{\tau_p k^2}{2\hbar^2} (\lambda_R \pm \lambda_D)^2. \quad (6)$$

The subscripts \pm denote the (110) and $(1\bar{1}0)$ orientation. An experimental procedure to measure spin lifetime

must therefore entail the direct substitution of C_v data in Eq. 6. Using Eq. 3, it is possible to write the Rashba coupling parameter in Eq. 6 as $\lambda_R \approx \sqrt{(4\alpha\Lambda E)/(1-\Lambda)}$, where $\Lambda = [1 - (12\alpha C_v)/(\pi k_B^2 T)]^2$. A proof is added to the supplementary material, Ref. 5.

The evaluation of Eq. 6 requires the momentum scattering time; the momentum scattering at low temperatures is primarily impurity scattering driven as the suppressed phonon modes contribute little to electron-phonon scattering. Taking this in to account, the imaginary part of the retarded self-energy (Σ) for the ensemble of conduction electrons whose motion is impeded by impurity sources, allows us to estimate the scattering time (τ_p) through the relation, $1/\tau_p = (2/\hbar) Im\Sigma$. The retarded self-energy in the self consistent Born approximation (SCBA) is expressed as a pair of equations¹⁸

$$G_{ks}(\epsilon) = \frac{1}{\epsilon - \epsilon_{ks} - \Sigma(\epsilon)}; \Sigma(\epsilon) = n_i v_i^2 \int \frac{d^2k}{4\pi^2} G_{ks}(\epsilon), \quad (7)$$

where n_i and v_i denote the density and strength of impurities, respectively and $G_{ks}(\epsilon)$ is the 2×2 retarded Green's function diagonal with respect to the band index s ($\langle s | G_k(\epsilon) | s \rangle = \delta_{ss'} G_{ks}(\epsilon)$). The retarded self-energy, Σ , in SCBA averaged over impurity distributions is also diagonal with respect to the band index s and independent of \mathbf{k} . Using the Green's function, $(E\mathbb{I} - H_{zb})^{-1}$, corresponding to the Hamiltonian in Eq. 1, the imaginary part of the retarded self-energy is

$$Im\Sigma(E) = \frac{n_i v_i^2}{8\pi} \int d^2k \left[(\delta_1 + \delta_2) \pm (\delta_1 - \delta_2) \right], \quad (8)$$

where δ_1 (δ_2) = $\delta(E - \alpha k^2 \mp \beta k)$. In deriving Eq. 8, the standard relation $\frac{1}{x \pm i\delta} = \mathbb{P}\frac{1}{x} \mp i\pi\delta(x)$ was used and as usual, the upper (lower) sign is for the spin-up (down) band. Evaluating this integral which closely resembles the one we encountered while computing the DOS, the retarded self-energy is approximately given as $n_i m^* v_i^2 / 4\hbar^2$ for both set of spin-chiral bands (see section on SCBA, Ref. 5). For an experimentally preset impurity density, $n_i = 1.0 \times 10^{11} \text{ cm}^{-2}$ and the attendant impurity potential¹⁹ being $0.1 \text{ keV}\text{\AA}^2$, the momentum scattering time for conduction electrons with effective mass equal to 0.0201 (obtained from a $k.p$ calculation for a 10.0 nm) wide well works out to roughly 5 ps. A sample calculation of spin lifetimes where the measured C_v is $5.2 \times 10^{-11} \text{ eV/K}$ (this is extracted for purpose of illustration from data presented in Fig. 3) gives τ_z as 5.68 ps while the lifetimes along the (110) and $(\bar{1}\bar{1}0)$ directions, τ_+ and τ_- , are 10.98 and 11.78 ps, respectively. A comment is in order here : Heat capacity is one of the several thermodynamic potentials that we have used in our analysis of spin lifetime. A similar estimation of the spin lifetime can be performed if we consider another thermodynamic potential, the Helmholtz free energy, defined as $F = U(T=0) - TS$, where $S = \int_0^T C_v/T' dT'$ is the

entropy. At two distinct temperatures, the difference between the Helmholtz free energies is $\Delta F = (T_2 - T_1) \Delta S$, where $\Delta S = 0.5(S_1 + S_2)$. The entropy S_i at temperature T_i , in the Sommerfeld expansion is identical to C_v .¹

To summarize, we have demonstrated the SOI-governed tunability of the electron heat capacity. The Rashba SOI, primarily, is adjusted utilizing dimensional confinement and mechanical strain. We have also shown that thermodynamic potential measurements offer an experimental technique to gauge the spin lifetimes. An application of our results that we did not discuss in the text is the computation of electronic thermal conductivity, $\kappa_e = C_v v_f^2 \tau_p / 3$, where v_f is the Fermi velocity. Going a step further, following the Wiedemann-Franz law which relates the thermal conductivity to electrical conductivity (σ) at low temperatures through the empirical relation, $\kappa/\sigma = LT$, where L is the Lorentz number, it is possible to evaluate the electrical resistivity ($1/\sigma$) from heat capacity measurements. Lastly, note that we have assumed $\lambda_R \neq \lambda_D$, however, the behaviour of the thermodynamic potentials under their equality hallmarked by the persistent spin helix^{20,21} and a much longer spin lifetime has not been examined.

- ¹G. Giuseppe and G. Paravicini, *Solid state physics* (Academic Press, Second Edition, 2013).
- ²M. Dressel and G. Gruner, *Electrodynamics of solids* (Cambridge University Press, 2002).
- ³Y. Wang, T. Plackowski, and A. Junod, *Physica C: Superconductivity* **355**, 179 (2001).
- ⁴R. Winkler, *Spin-Orbit Coupling in Two-Dimensional Electron and Hole Systems* (Springer, 2003).
- ⁵"Supplementary material."
- ⁶E. d. A. e Silva, G. La Rocca, and F. Bassani, *Physical Review B* **50**, 8523 (1994).
- ⁷G. Bastard, *Wave mechanics applied to semiconductor heterostructures* (Wiley-Interscience, 1991).
- ⁸I. Vurgaftman, J. Meyer, and L. Ram-Mohan, *Journal of applied physics* **89**, 5815 (2001).
- ⁹K. Ishizaka, M. Bahramy, H. Murakawa, M. Sakano, T. Shimojima, T. Sonobe, K. Koizumi, S. Shin, H. Miyahara, A. Kimura, *et al.*, *Nature materials* **10**, 521 (2011).
- ¹⁰A. Manchon, H. Koo, J. Nitta, S. Frolov, and R. Duine, *Nature materials* **14**, 871 (2015).
- ¹¹A. Syro, F. Fortuna, C. Bareille, T. Rödel, G. Landolt, N. Plumb, J. Dil, and M. Radović, *Nature materials* **13**, 1085 (2014).
- ¹²X. Zhang, Q. Liu, J. Luo, A. Freeman, and A. Zunger, *Nature Physics* **10**, 387 (2014).
- ¹³P. Sengupta, H. Ryu, S. Lee, Y. Tan, and G. Klimeck, *Journal of Computational Electronics* **15**, 115 (2016).
- ¹⁴W. Zawadzki and P. Pfeffer, *Semiconductor Science and Technology* **19** (2003).
- ¹⁵"See, for e.g., Ch. 9 in *The physics of dilute magnetic alloys*; J. Kondo. Cambridge Univ. Press (2012)."
- ¹⁶I. Žutić, J. Fabian, and S. D. Sarma, *Reviews of modern physics* **76**, 323 (2004).
- ¹⁷N. Averkiev, L. Golub, and M. Willander, *Journal of physics: condensed matter* **14**, R271 (2002).
- ¹⁸C. Di Castro and R. Raimondi, *Statistical Condensed Matter Physics* (Cambridge University Press, 2015).
- ¹⁹P. Sengupta and E. Bellotti, *Appl. Phys. Letters* **108**, 211104 (2016).
- ²⁰P. Sengupta and E. Bellotti, *Appl. Phys. Letters* **108**, 031101 (2016).
- ²¹M. Liu, K. Chen, S. Chen, and C. Chang, *Physical Review B* **74**, 235322 (2006).